Comparison of Internal Hydrogen Embrittlement of Superalloys 718 and 625

Peter D. Hicks* and Carl J. Altstetter**

* Argonne National Laboratory, 9700 S. Cass Avenue, Argonne, 60439, Illinois, USA
** Department of Materials Science and Engineering ,University of Illinois, 1304 W. Green Street, Urbana, 61801, Illinois, USA

Abstract

Mechanical tests were used to compare the internal hydrogen embrittlement susceptibility of alloy 718 to that of alloy 625. Slow, constant extension rate tests (CERT), on edge-notched strip specimens were performed at 25°C for alloy 718 (both aged and annealed) and alloy 625 (annealed). The results for internal hydrogen were compared to those for (i) 101 kPa external gaseous hydrogen environments, and (ii) dynamic cathodic charging at current densities up to 1000 A/m^2 in a 0.7 M H_2SO_4 plus 1 g/l of $NaAsO_2$ solution. Hydrogen precharging was carried out at 250°C in a molten salt bath for times sufficient to produce uniform hydrogen concentrations up to 50 wt ppm H (0.3 atomic %). Subcritical crack growth (SCG) rates at constant load also were measured on aged 718 and annealed 625. Fractographic features for various testing environments and internal hydrogen contents were compared for the two alloys. Both were found to be susceptible to internal hydrogen embrittlement as evidenced by decreases in notch tensile strength, reduction of area and threshold stress intensity for subcritical crack growth. Microscopic evidence suggests that hydrogen enhanced the localization of plasticity and led to planar slip and finally failure.

Superalloys 718, 625 and Various Derivatives
Edited by Edward A. Loria
The Minerals, Metals & Materials Society, 1991

Introduction

Internal hydrogen may be present in alloys from a variety of sources, not only from their use in hydrogen gas, but many of them related to processing (hydrogen retained after casting, pickling, welding, electroplating, etc.). Another source of hydrogen is corrosion reactions: In the presence of water the cathodic counterpart of the corrosion reaction is the liberation and deposition of atomic hydrogen. The effects of internally absorbed hydrogen can be observed long after the sources have been removed, leading to delayed failure[1,2]. Delayed failure can be avoided by eliminating sources of hydrogen, or reducing its level to a harmless value by using improved processing techniques. However, the possibility of accumulating large internal concentrations of hydrogen still exists when the alloy is used in strongly acidic solutions or in the presence of hydrogen-containing gases for times sufficient to allow hydrogen diffusion into the metal.

For the case of superalloys 718 and 625 the majority of hydrogen embrittlement studies have been concerned with hydrogen environment embrittlement[3-17] and they were mostly for the purpose of alloy evaluation and comparison of basic mechanical properties of these alloys in H_2 versus He environments. Both alloys are susceptible to external gaseous hydrogen embrittlement under certain conditions, with alloy 718 more embrittled than alloy 625 under the same conditions. In a study performed by Gray[13] it was shown that alloy 718 is also slightly susceptible to internal hydrogen embrittlement, although his tests only included hydrogen concentrations up to about 3 wt ppm.

The majority of the gaseous hydrogen environment (GHE) studies performed to date have been carried out at hydrogen pressures well above atmospheric pressure. It was therefore decided to investigate the GHE susceptibility of these two alloys at atmospheric pressure. Additional tests used dynamic cathodic charging i.e., aqueous cathodic charging of hydrogen during constant extension rate (CERT) testing to give a very high local hydrogen fugacity at the specimen surfaces. This simulates the susceptibility of these alloys to GHE at pressures greater than those used in previous research. The largest part of this research utilized hydrogen precharging in molten salt to study internal hydrogen embrittlement and to compare the failure processes with those in a hydrogen environment. It was intended to try to understand the role of microstructure on the mechanical behavior of alloys 718 and 625 with a known internal hydrogen concentration.

A detailed description of hydrogen embrittlement mechanisms will not be given in this paper, so for further details on these mechanisms readers are advised to consult references[3,18-43]. The authors present a more detailed discussion of embrittlement mechanisms for alloys 718 and 625 in references[44-46].

Experimental Procedure

The test material was supplied in the mill-annealed condition by the Allegheny Ludlum Steel Corporation. The chemical compositions

of the two alloys are given in table I.

Table I: Composition of alloys in weight percent.

	718	625		718	625
Cr	18.3	20.3	Si	0.15	0.22
Ni	bal.	bal.	Mn	0.11	0.13
Mo	3.02	8.22	Cu	0.05	0.09
Nb	5.07	3.26	Co	0.42	0.07
Ti	1.00	0.18	C	0.044	0.036
Al	0.63	0.19	N	0.007	0.013
V	0.008	-	B	0. 004	-
Fe	18.50	4.49	P	0.008	0.009
			S	0.001	0.0005

Mill-annealing temperatures were: 980°C (alloy 718) and 1065°C (alloy 625). The material was supplied in long strips, approximately 1.5 mm thick and 25 mm wide. For all of the mechanical tests 150 mm long strips were used with the rolling direction lengthwise. Alloy 718 was further aged to yield the maximum tensile properties[47]: Annealed at 1066°C for 1 hr under a vacuum of approximately 10 Pa, air cooled, aged in vacuum at 760°C for 10 hrs, furnace cooled to 650°C for a further 10 hrs (giving a total aging time of 20 hrs) followed by air cooling. Mechanical testing indicated and transmission electron microscopy (TEM) verified the presence of the desired γ' and γ'' precipitates. Alloy 625 was used in the as-received condition.

After heat treating, all strips were ground on 300 grit abrasive paper and then electropolished (15-30 volts in a 20% H_2SO_4: 80% methanol solution at 0°C). GHE tests were performed on both alloy 718 and alloy 625 in the annealed condition and on aged 718. A 300 μm thick diamond saw blade was used to make a notch of about 7 mm in depth at the mid-point of one edge of the specimens, giving a notch root radius of about 150 μm. For the GHE tests, the notch region was encapsulated by sealing to it a plastic tube which was evacuated prior to introduction of a stream of high purity hydrogen gas. The dynamic cathodic charging tests were performed by filling the container with 0.7 M H_2SO_4 plus 1 g/l $NaAsO_2$ solution. A current density of up to 1000 A/m^2 was then applied between the specimen and a platinum anode[45]. Homogeneous hydrogen charging prior to testing was done at 250°C, in a molten salt consisting of a 1:1 molar ratio of KOH and NaOH through which moisture saturated N_2 gas was bubbled[44]. It was found that varying the voltage between the specimen and a nickel anode gave reproducible, uniform hydrogen concentrations between 0 and 50 wt ppm. Hot vacuum extraction and volumetric measurement was used for dissolved hydrogen gas determinations.

For the CERT tests specimens were held in wedge grips and pulled at a cross head speed of 8.5×10^{-7} m/s. In the case of the 101 kPa hydrogen pressure test, the CERT test was begun at the same time as the hydrogen was passed through the test cell. In the dynamic cathodic charging experiments the CERT test was started as soon

as the cathodic current was applied. For both of the above tests temperatures of 25 and 50°C were used. In all cases crack extension started only after the maximum load was reached. Both alloys also exhibited continuous yielding under all conditions tested. Percent reduction of area (RA) and notch tensile strength (NTS, defined as the maximum load divided by the original net section area) were used to quantify hydrogen embrittlement during the CERT tests. SEM observations were performed on all fracture surfaces.

Subcritical crack growth (SCG) tests were performed only on precharged specimens of aged 718 and annealed 625 (commonly used engineering conditions). Additional CERT tests were run at 25°C only, while SCG tests were run at 0, 25 and 50°C. A few SCG tests were run at 75 and 100°C for aged alloy 718. The SCG specimens were the same as the CERT specimens except that an additional 1 mm of fatigue precracking (stress ratio of 0.3) was performed after precharging and specimen notching. The peak load during fatigue precracking was of the order of 60% of the load required for SCG. Details of the procedure for performing the SCG tests and the data reduction are described elsewhere[45,46]. Basically a constant load was incremented daily until the crack grew more than 30 μm in a day's time. The crack position was then measured at various time intervals with an optical microscope. The stress intensity was calculated from $K=Y\sigma\sqrt{a}$, where σ is the remote stress, a is the total crack length (including notch) and Y is a geometric factor given by[48]:

$$Y = 1.99 - 0.41(Z) + 18.7(Z)^2 - 38.48(Z)^3 + 53.85(Z)^4$$

where Z = a/W, W is the width of the specimen (≈25 mm). For the specimen geometry used in the above investigation, plane stress conditions would be expected, however in the embrittled condition very little specimen thinning occurred. The threshold stress intensity (K_{th}) was defined as that below which the SCG rate did not exceed 30 μm per day (3.5×10^{-11} m/s).

Results

Microstructure. In the as-received condition, alloys 718 and 625 had grain sizes of about 10 μm, while in the peak aged condition alloy 718 had a grain size of 30 μm (due to grain growth during the final anneal). Titanium and niobium carbides were identified as the major particles, present both within the grains and as grain boundary particles. Carbide stringers, elongated in the rolling direction, lay perpendicular to the crack growth direction in all cases.

Constant Extension Rate Tests. Table II gives the NTS and RA data for both alloys, tested in air at room temperature (25°C ±2°C). Results are averages of three tests, with the results of each test not deviating by more than 5% from the mean. The results are identical in a 101 kPa H_2 environment. Also, at 50°C the GHE test results are unchanged from the RT (room temperature) CERT results. Thus the low pressure external hydrogen gas environment did not embrittle these alloys, and the fracture surface was

dimpled, characteristic of microvoid coalescence (MVC)(Fig. 1).

Table II: Effect of dissolved hydrogen on RA (%) and NTS (MPa) for alloys 718 and 625. CERT tested in air at 25°C.

Alloy (condition)	0 wt ppm Hydrogen		% Decrease due to 40 wt ppm Hydrogen	
	RA(%)	NTS(MPa)	RA	NTS
IN718 (aged)	22	1017	67	33
IN718 (annealed)	31	552	16	7
IN625 (annealed)	40	559	29	13

During the dynamic cathodic charging experiments profuse, shallow tensile cracks were observed on the side surfaces of the specimens, Fig. 2. The tensile crack depth was found to be a function of the applied cathodic current density, Fig. 3, and it was the same for both alloys. After completion of the test and after hydrogen outgassed from the surfaces, craze cracking was observed on the faces and on the fracture surfaces, Fig. 4. This cracking was found to be of both the inter- and transgranular type. The fractographic features on the remaining 80 - 100% of the fracture surface were unaffected by this cathodic charging, and the CERT properties of both of the alloys were essentially unaffected by this high hydrogen fugacity at the specimen surface. Varying the temperature from 25 to 50°C also had no noticeable effect on the extent of this cracking, or on the mechanical properties.

For the hydrogen precharged specimens, Figs. 5 and 6 show the RA and NTS, respectively, versus the bulk hydrogen content in wt ppm. Each point is the average of two tests, with each result not varying by more than 5% from the mean value. In all cases the ductility and strength decreased with the dissolved hydrogen content. Table II shows the percentage decreases in RA and NTS due to the addition of 40 wt ppm of hydrogen to these alloys. It can be seen that while aged 718 shows the greatest susceptibility to embrittlement, annealed 718 is degraded the least by dissolved hydrogen. For both alloys, it was found that as the dissolved hydrogen content increased, the fracture surface showed a greater proportion of {111} planar facets (Fig. 7). For alloy 718 the entire fracture surface consisted of these {111} facets for the higher dissolved hydrogen contents (>32 wt ppm H). The surfaces of alloy 625 (42 wt ppm H) showed isolated regions of these facets dispersed amongst regions of dimpled failure. This was similar to 718 fracture surfaces for a dissolved hydrogen content of 19 wt ppm, for example, Fig. 8. These facets are not true brittle facets (showing "river patterns", for example), but were seen to be sheets of microdimples, showing extensive localized plasticity[46].

Subcritical Crack Growth Rate Tests. All of the SCG rate tests on hydrogen precharged specimens were performed in air because it was found that no SCG behavior was exhibited by any of the alloys

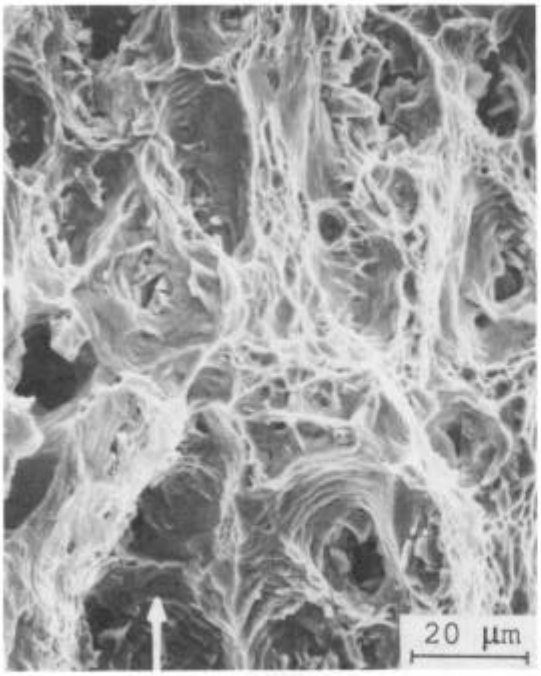

Figure 1: Fracture surface, after CERT test, of alloy 718 (aged), 0 wt ppm H. Arrow indicates crack propagation direction in all of the micrographs.

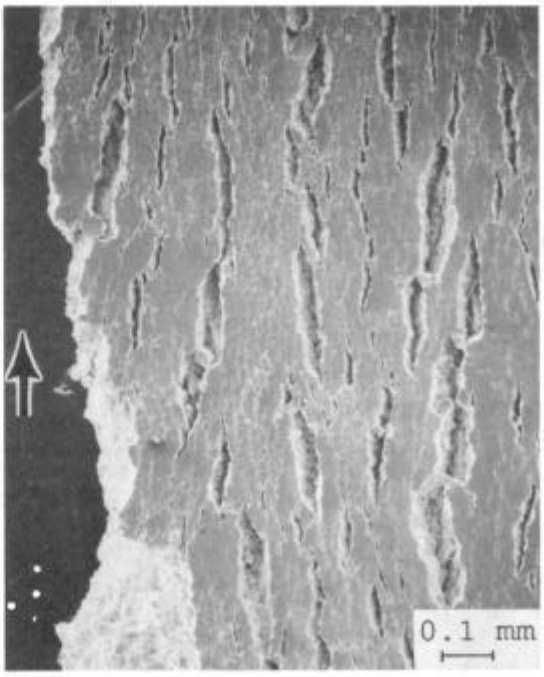

Figure 2: Alloy 718 (aged). CERT tested with dynamic cathodic charging at 200 A/m². Tensile cracking as viewed on the specimen side-surface, below the fracture surface.

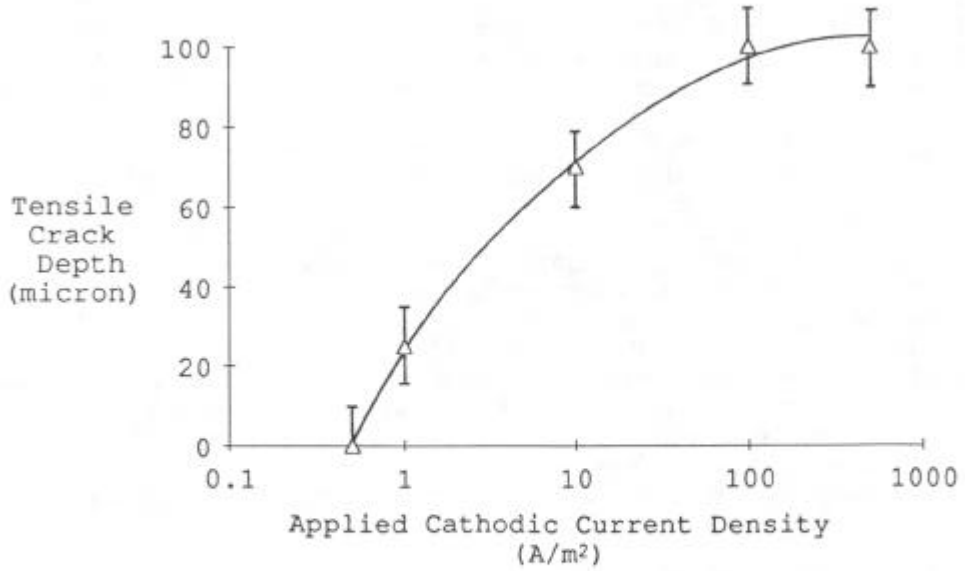

Figure 3: Tensile crack depth in alloy 718 and 625 as a function of current density during a dynamic cathodic charging CERT test.

Figure 4: Cracking at the outer edge of the fracture surface for alloy 625, charged at 200 A/m².

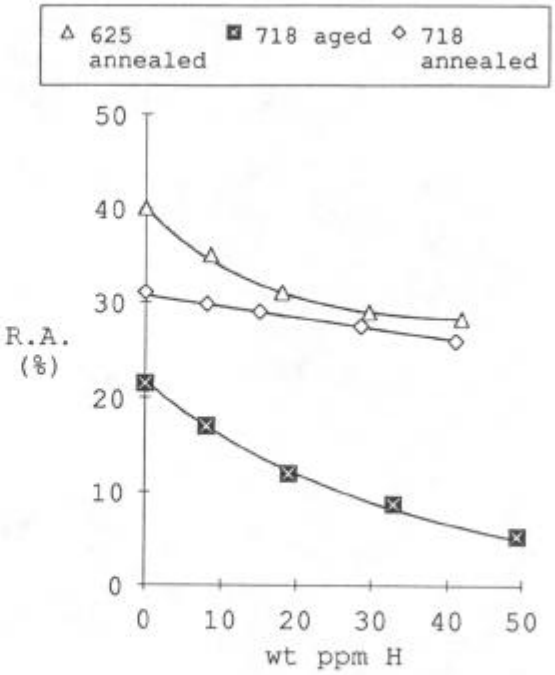

Figure 5: Reduction of area (RA) as a function of the dissolved hydrogen content for 25°C CERT tests.

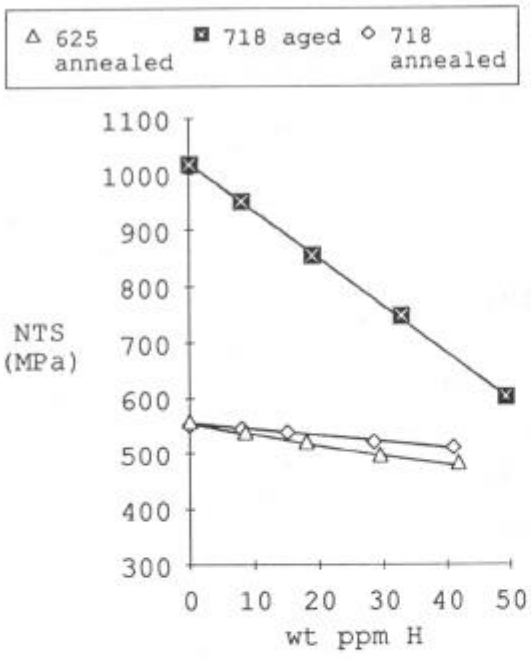

Figure 6: Notch tensile strength (NTS) as a function of the dissolved hydrogen content for 25°C CERT tests.

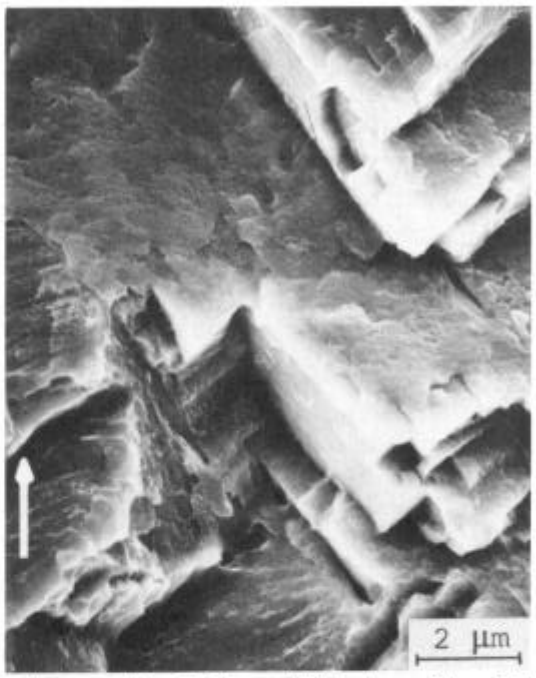

Figure 7: Alloy 718 (aged), 33 wt ppm H. CERT tested at 25°C.

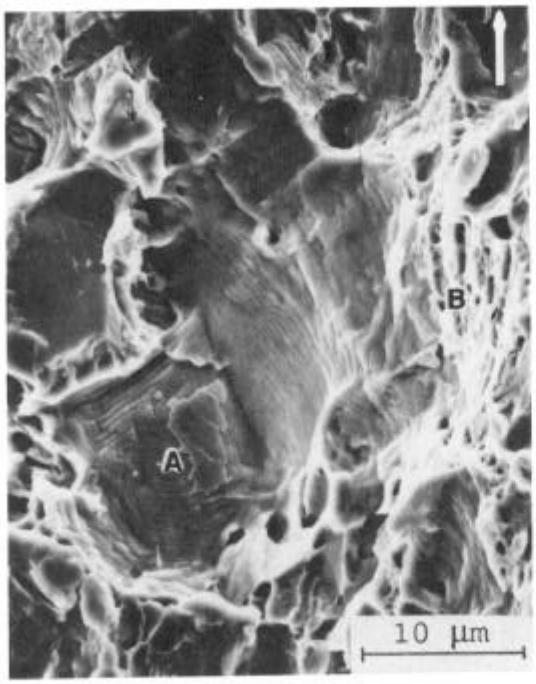

Figure 8: Alloy 718 (aged), 19 wt ppm H. Fracture surface consists of flat facets (A) and small, flat dimpled areas separated by tear ridges (B).

in 101 kPa H_2. It was also shown that testing hydrogen precharged specimens at 25°C in air gave the same SCG behavior as for testing that same precharged specimen in a 101 kPa H_2 gas environment. Figures 9 and 10 show typical crack growth rate (da/dt) curves obtained for alloys 718 and 625, respectively, at 0°C. The flat, stress intensity-independent regions are referred to as stage II of SCG. In general for alloy 718, stage II, when observed, lasted for only several hundred microns of crack growth. On the other hand, stage II cracking in alloy 625 corresponded to stable crack advance for up to 1 mm before rapid, unstable crack growth was followed by complete failure. Figures 11 and 12 show that the threshold stress intensities, K_{th}, decreased with temperature and dissolved hydrogen content.

For aged alloy 718 at higher dissolved hydrogen contents, the curves levelled off, and a few tests at 75°C and 100°C yielded data points which fell on the 50°C curve. For alloy 625, Fig. 12, there was no tendency for the effect of the hydrogen to saturate. Figure 13 shows that the stage II crack growth rate was a linear function of the square of the dissolved hydrogen content, for both alloys at both 0 and 50°C.

The SCG fracture surfaces were similar to the fracture surfaces observed for comparable hydrogen concentrations in the CERT tests[46]: For alloy 718 with a few ppm of hydrogen the fracture surface was dimpled. Isolated facets of {111} planar failure were seen in stage II SCG and became greater in number as the hydrogen content increased. For the higher dissolved hydrogen contents where stage II SCG begins to disappear (>12 wt ppm H) the fracture surface consists exclusively of {111} planar facets. For alloy 625, all of stage II consisted of dimples. Larger dimples are associated with carbide rich regions and the fractured carbides lie at the base of the dimples, while smaller dimples are found in the carbide deficient regions. Regions of {111} planar facetting were observed only for the higher dissolved hydrogen contents (>16 wt ppm H), where stage II of SCG began to disappear[46].

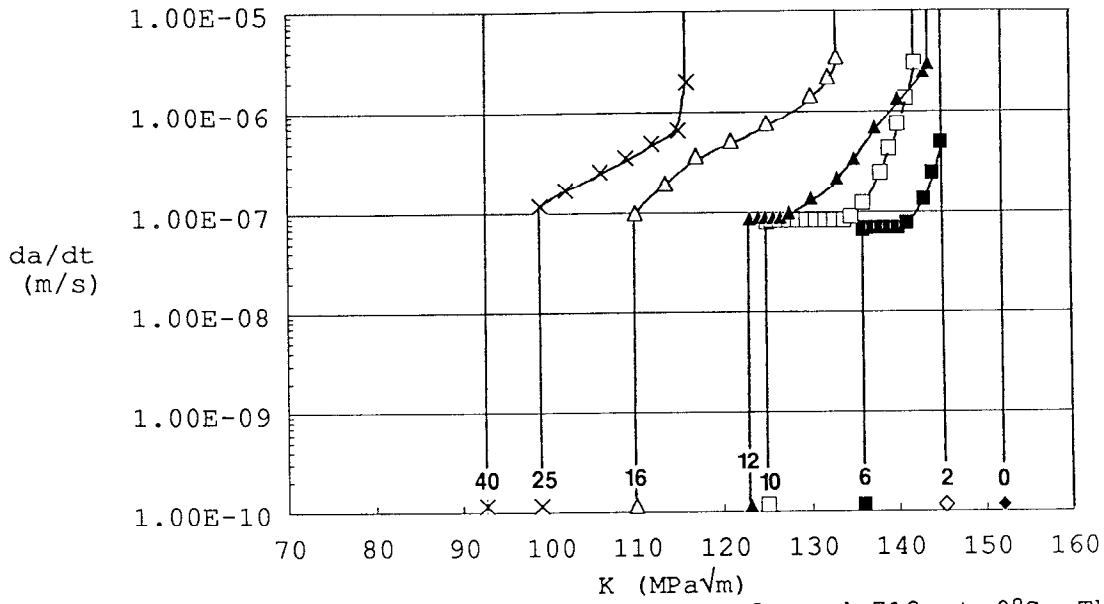

Figure 9: Subcritical crack growth rate of aged 718 at 0°C. The curves are labelled with the hydrogen concentration in wt ppm.

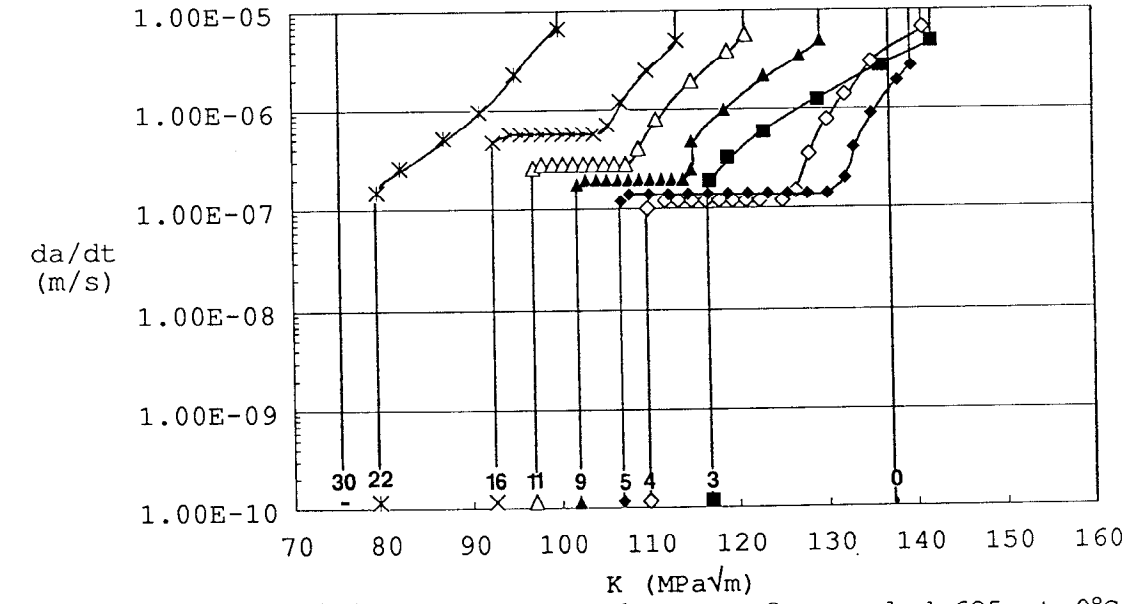

Figure 10: Subcritical crack growth rate of annealed 625 at 0°C. The curves are labelled with the hydrogen concentration in wt ppm.

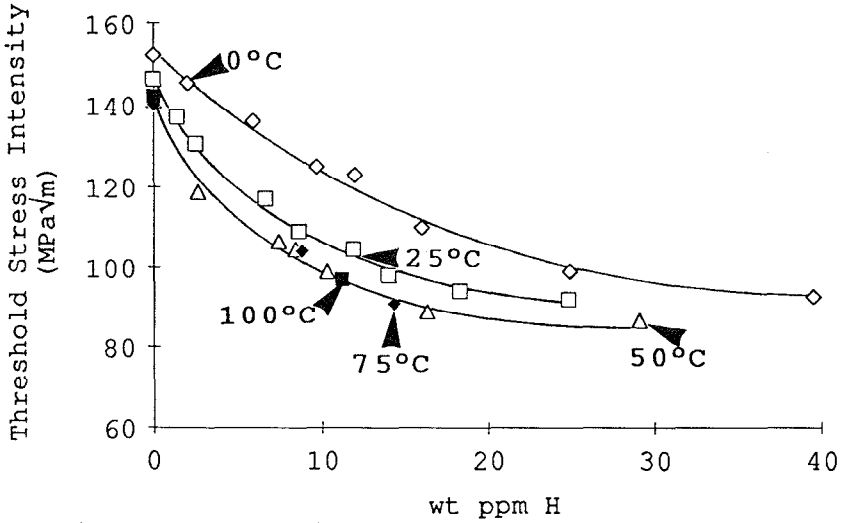

Figure 11: K_{th} vs. dissolved hydrogen content, for aged alloy 718, SCG tested at 0°C, 25°C, 50°C, 75°C and 100°C.

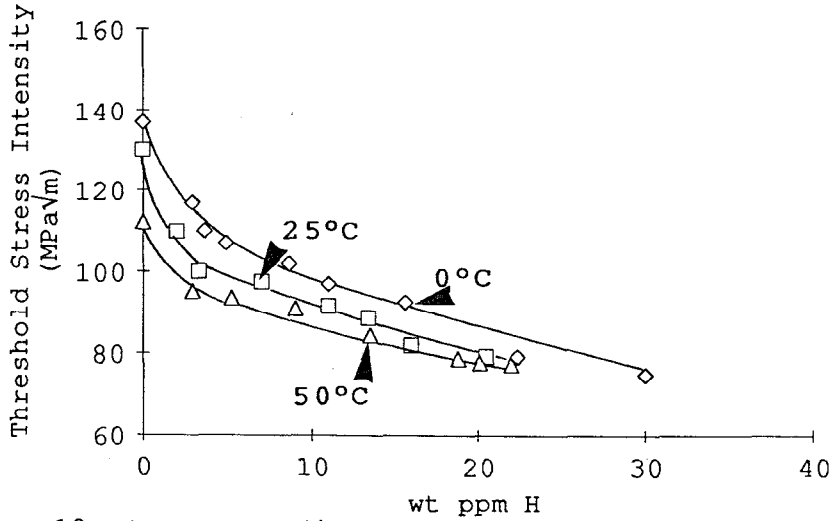

Figure 12: K_{th} .vs. dissolved hydrogen content, for annealed alloy 625, SCG tested at 0°C, 25°C and 50°C.

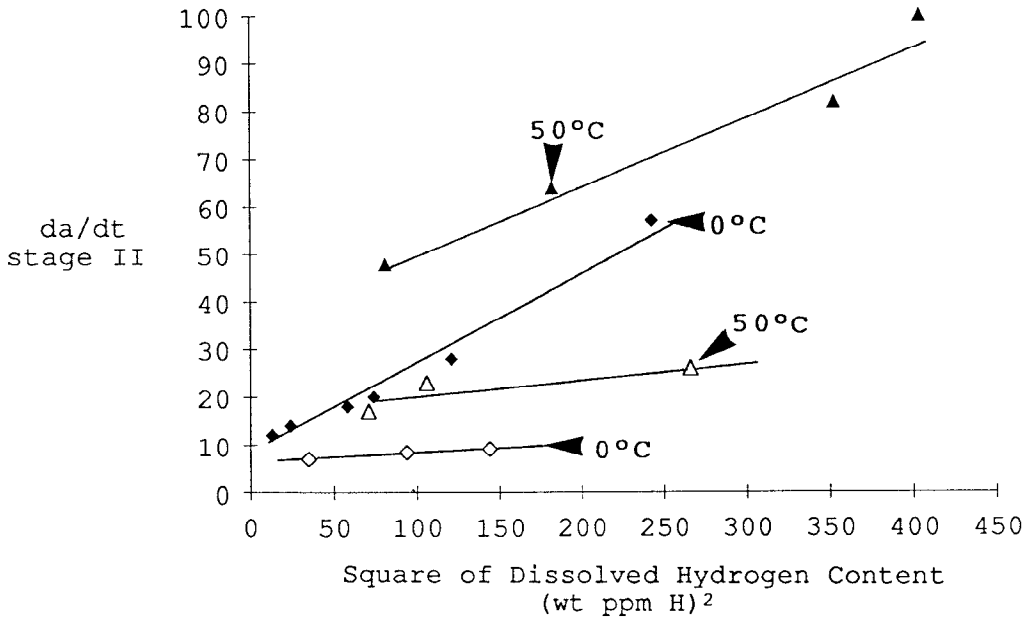

Figure 13: Subcritical crack growth rate in stage II vs. the square of the dissolved hydrogen content for aged alloy 718 (open symbols) and annealed alloy 625 (filled symbols), at 0°C and 50°C.

Discussion

It has been shown that the source of hydrogen, the material and its microstructure, the test technique, specimen configurations and sizes, etc, play an important role in determining whether alloys 718 and 625 are embrittled by hydrogen. Much of the earlier work showed that both of these alloys are embrittled to various degrees, in gaseous hydrogen environments up to pressures of 70 MPa. It is clear that none of the alloys were embrittled by 101 kPa H_2 environments. Much higher hydrogen fugacities lead to severe, localized surface cracking, both during and after the CERT tests. The cracking that appeared after the tests is thought to be associated with biaxial tensile stresses set up during the decomposition of a surface hydride layer[49-54]. At the proper combination of strain rate (crack growth rate) and applied stress in relation to hydrogen diffusivity and hydrogen fugacity the cracking is limited to the specimen surfaces, leaving the sample central regions unaffected by this external hydrogen environment.

For the internally charged specimens of both alloys, up to 50 wt ppm H, there was no effect of the dissolved hydrogen on the Young's modulus or the 0.2% yield stress, but it is apparent that dissolved hydrogen reduced the RA and NTS for aged alloy 718 and annealed alloys 718 and 625. Sufficient dissolved hydrogen also led to SCG at constant load, and K_{th} decreased as the hydrogen concentration increased. Other observations[46] lead us to believe

that hydrogen-enhanced localization of plasticity is the mechanism that best describes the embrittlement of these alloys. There is evidence[46] indicating a diminished capacity for general plasticity, yet there is ample evidence for local plasticity. The local plasticity is confined to bands of {111} planes where the density of localized dislocation activity is high ({111} are the slip planes in these alloys). In both alloys the {111} fracture surface facets become more pronounced as the dissolved hydrogen content increased. The reason for the greater preponderance of {111} planar failure in aged alloy 718 vs. the annealed alloys 718 and 625, for the same dissolved hydrogen content, is that even in hydrogen-free material planar slip is enhanced in the aged alloy by the presence of fine precipitates[46] which give rise to slip channeling[55]. Final, ductile, micro-dimpled failure then took place within the {111} planar deformation bands instead of larger, macroscopic dimple formation, which requires plasticity over a larger volume. For a more detailed discussion on the mechanisms of failure refer to the references[46,56,57]. It is also worth noting that during the fatigue precracking of the highly charged alloys (>30 wt ppm H in the case of aged alloy 718), the fracture morphology changed from ductile fatigue striated failure (low dissolved hydrogen contents) to {111} planar fracture facets. This further indicates that the preferred mode of failure at the higher dissolved hydrogen contents is one which involves less overall plasticity, but still plenty of localized microplasticity.

In general, face centered cubic alloys such as alloys 718 and 625 have much greater resistance to hydrogen effects than body centered cubic steels of comparable strength[58]. These austenitic alloys have high hydrogen solubilities and low hydrogen diffusivities, which necessitate excessively long exposure times to high pressure hydrogen gas, at temperature, in order to achieve uniformly high dissolved hydrogen concentrations in thick specimens. The solubility of hydrogen in alloy 718 is given by[59]:

$$S = 8.8\exp[-8.1(\text{kJ/mole})/RT](\text{wt ppm H/atm}^{1/2})$$

So, for example, a temperature of 300°C and a hydrogen pressure of about 975 atmospheres would be needed to achieve a solubility of 50 wt ppm H. It would therefore be uncommon that the highest dissolved hydrogen contents used in this research would be found in current engineering practice by hydrogen gas alone. However, high hydrogen fugacities generated during corrosive processes could lead to considerable hydrogen absorption by these alloys. Clearly though, only several wt ppm H need be absorbed to start to embrittle these alloys.

In the case of alloy 625 the presence of MVC during stage II of SCG can be explained by void pressurization[46], but probably of greater engineering significance is that there was very little stable crack growth once K_{th} was exceeded. This was true for both alloys. It appears that the decrease in K_{th} is commensurate with the decrease in NTS for these alloys. Cracking simply initiates and propagates at lower stresses when hydrogen is present in a sufficient quantity.

Conclusions

• Aged alloy 718 and annealed alloys 718 and 625 are susceptible to both gaseous hydrogen environment and internal hydrogen embrittlement. The severity of internal hydrogen embrittlement was seen to increase with dissolved hydrogen contents, up to 50 wt ppm H, as evidenced by decreases in %RA, NTS and K_{th} values.

• Increasing dissolved hydrogen contents results in fractographic changes from dimpled failure at low dissolved hydrogen contents to {111} planar facets for the higher dissolved hydrogen contents (up to 50 wt ppm H). This was seen under CERT, SCG and fatigue conditions.

• The greater susceptibility to hydrogen embrittlement of aged 718 vs. the annealed alloys is explained by hydrogen enhanced localization of plasticity as the operative mechanism for hydrogen embrittlement. The effect of hydrogen was to accentuate slip channeling in aged superalloy microstructures.

Acknowledgements

The authors gratefully acknowledge: the Allegheny Ludlum Steel Corporation for providing the alloys and their chemical compositions, the National Science Foundation for funding this research under contract NSF DMR 86-05955, the Department of Materials Science and Engineering at the University of Illinois for co-sponsoring the research, and the Materials Research Laboratory at the University of Illinois for the use of their microstructural analysis facilities.

References

1. R.P. Frohmberg, W.J. Barnett and A.R. Troiano: Trans. ASM, Vol. 47, 1955, pg. 892.

2. A.R. Troiano: Trans. ASM., Vol. 52, 1960, pg. 54-80.

3. R.P. Jewett, R.J. Walter, W.T. Chandler and R.P. Frohmberg: "Hydrogen Environment Embrittlement of Metals". NASA CR-2163, March 1973.

4. R.J. Walter and W.T. Chandler: "Effects of High Pressure Hydrogen on Metals at Ambient Temperature". Final report on contract NAS8-19, Report R-7780-1,2,3. 1969. Rocketdyne.

5. R.J. Walter, R.P. Jewett and W.T. Chandler: "On the Mechanism of Hydrogen Environment Embrittlement if Iron and Nickel Base Alloys". Mat. Sci. Eng., Vol. 5, 1969/70, pgs. 98-110.

6. R.J. Walter and W.T. Chandler: "Effect of Hydrogen Environments on Inconel 718 and Ti-6Al-4V (STA)". Paper presented at AIME meeting, Las Vegas, Nevada, May 11-14, 1970.

7. R.J. Walter and W.T. Chandler: "Effect of Hydrogen Environment on Inconel 718 and Ti-6Al-4V Under Simulated J-2 Engine Operating Environments". Report R-7920, Rocketdyne.

Contract NAS8-19C, NASA, MSFC, Huntsville, Alabama, 30 June 1969.

8. R.J. Walter and W.T. Chandler: "Effect of High Pressure Hydrogen on Inconel 718 at -260°F". Research Report RR 70-3, Rocketdyne, Canoga Park, California, 1 June 1970.

9. P.M. Lorenz: "Effect of Pressurized Hydrogen upon Inconel 718 and 2219 Aluminum". Boeing Document D2-114417-1, The Boeing Company, Seattle, Washington, February 1969.

10. R.J. Walter and W.T. Chandler: "Metallography of Alloys Fractured in Gaseous Hydrogen Environments". Paper presented at AIME meeting, Las Vegas, Nevada, 11-14 May 1970.

11. E.J. Bachelet and A.R. Troiano: "Hydrogen Gas Embrittlement and the Disc Pressure Test". NASA CR-134551, November 30, 1973.

12. V. Frick, G.R. Janser and J.A. Brown: "Enhanced Flaw Growth in SSE Main Engine Alloys in High Pressure Gaseous Hydrogen". Proceedings of National Space Technical Conference: "Space Shuttle Materials", 1971, held in Huntsville, Alabama. pgs. 597-634.

13. H.R. Gray: "Embrittlement of Nickel-, Cobalt-, and Iron-base Superalloys by Exposure to Hydrogen". NASA TND-7805, October 1974, 44 pgs.

14. J.A. Harris and J. Mucci: "Influence of Gaseous Hydrogen on the Mechanical Properties of High Temperature Alloys". NASA CR 149962, July 1976.

15. J.A. Harris and M.C. van Wanderham: "Properties of Materials in High Pressure Hydrogen at Cryogenic, Room and Elevated Temperatures". 31 July 1973, NAS8-26191.

16. R.D. Kane: "Accelerated Hydrogen Charging of Nickel and Cobalt Base Alloys". Corrosion, Vol. 34, 1978, pgs. 442-445.

17. R.D. Kane, M. Watkins, D.F. Jacobs and G.L. Hancock: "Factors Influencing the Embrittlement of Cold Worked High Alloy Materials in H_2S Environments". Corrosion, 1977, pgs. 309-320.

18. M.R. Louthan Jr., C.R. Caskey, J.A. Donovan and D.E. Rawl, Jr.: "Hydrogen Embrittlement of Metals". Mat. Sci. and Eng., Vol. 10, 1972, pgs. 289-300.

19. C.A. Zapffe: Mater. Methods, Vol. 32, 1950, pg. 58.

20. A.S. Tetelman and W.D. Robertson: Acta Met., Vol. 11, 1963, pg. 415.

21. J.K. Tien, S.V. Nair and R.R. Jensen: "Dislocation Sweeping of Hydrogen and Hydrogen Embrittlement", Hydrogen Effects in Metals, I.M. Bernstein and A.W. Thompson, editors. TMS, Warrendale, 1981, pgs. 37-53.

22. R.A. Oriani and P.H. Josephic: Acta. Met., Vol. 22, 1974, pgs. 1065-1074.

23. G.G. Hancock and H.H. Johnson: Trans. AIME, Vol. 236, 1966, pg. 207.

24. H.H. Johnson and J.P. Hirth: "Internal Hydrogen Supersaturation Produced by Dislocation Transport". Met. Trans. A., Vol. 7A, 1976, pgs. 1543-1548.

25. R.A. Oriani and P.H. Josephic: Acta Met., Vol. 25, 1977, pg. 979.

26. R.A. Oriani: Ber. Bunsenges. Phys. Chem., Vol. 76, 1972, pg. 848.

27. R. Thomson: "Brittle Fracture in a Ductile Material with Application to Hydrogen Embrittlement". J. Mat. Sci., Vol. 13, 1978, pgs. 128-142.

28. C.J. McMahon, Jr, C.L. Briant and S.K. Banerji: in: "Fracture", 1977, Vol. 1, pg. 363.

29. C.D. Beachem: Met. Trans. 1972, Vol. 3A, pg. 437.

30. N.J. Petch and P. Stables: Nature, Vol. 169, 1952, pg. 842.

31. N.J. Petch: Phil. Mag. Vol. 1, 1956, pg. 331.

32. J. Clum: Scripta. Met., Vol. 9, 1975, pg. 51.

33. S.P. Lynch and N.E. Ryan: in "Hydrogen in Metals". Proc. of 2nd International Congress, Paris, June 1977, Oxford 1978 (Pergamon Press), Paper 3D12.

34. H. Matsui, H. Kimura and S. Moriya: Mater. Sci. Eng. Vol. 40, 1979, pg. 207.

35. R.M. Latanision and R.W. Staehle: Acta. Met., Vol. 17, 1969, pg. 307.

36. J. Eastman, T. Matsumoto, N. Narita, F. Heubaum and H.K. Birnbaum: "Hydrogen Effects in Nickel-Embrittlement or Enhanced Ductility". The Effect of Hydrogen on the Behavior of Materials, I.M. Bernstein and A.W. Thompson, editors. TMS, Warrendale, 1981, pgs. 397-409.

37. I.M. Robertson and H.K. Birnbaum: "Effect of Hydrogen on the Dislocation Structure of Deformed Nickel". Scripta. Met., Vol. 18, 1984, pg. 269-274.

38. I.M. Robertson, T. Tabata, W. Wei, F. Heubaum and H.K. Birnbaum: "Hydrogen Embrittlement and Grain Boundary Fracture". Scripta. Met., Vol. 18, 1984, pg. 841-846.

39. H.K. Birnbaum: "Hydrogen Related Fracture of Metals", Atomistics of Fracture. R.M. Latanision and J.R. Pickens,

editors. Plenum Press, New York, 1981, pgs. 733-764.

40. S. Gahr, M.L. Grossbeck and H.K. Birnbaum: Acta. Met. Vol. 25, 1977, pg. 125.

41. H.K. Birnbaum: "Mechanisms of Hydrogen-Related Fracture of Metals". Technical report to ONR on contract USN 00014-83-K-0468, May 1989.

42. P. Bastien and P. Azou: Proc. First World Metallurgical Congress, ASM, Cleveland, 1951, pg. 535-552.

43. M.R. Louthan, Jr., G.R.Caskey, Jr., J.A. Donovan and D.E.Rawl, Jr.: Mater. Sci. Eng., Vol. 10, 1972, pg. 357-368.

44. P.D. Hicks and C.J. Altstetter: "Internal Hydrogen Effects on Tensile Properties of Iron and Nickel-Base Superalloys". Met. Trans. A., Vol. 21A, Feb. 1990, pgs. 365-372.

45. P.D. Hicks and C.J. Altstetter: "Hydrogen Embrittlement of Superalloys". Hydrogen Effects on Material Behavior. N.Moody and A Thompson, editors. TMS, Warrendale, 1990, pgs. 613-623.

46. P.D. Hicks and C.J. Altstetter: "Hydrogen-enhanced Cracking of Superalloys" Submitted for publication in Metallurgical Transactions.

47. Aerospace Structural Metals Handbook. 1980 Publication (Formerly AFML-TR-68-115). Daniel.J. Maykuth (Tech. Editor). Mechanical Properties Data Center, Battelle, Columbus Laboratories. Obtainable from: Department of Defence, Technical Monitoring by Army Materials and Mechanics Research Center, Watertown, Massachusetts, 02172, USA.

48. W.F. Brown Jr and J.E. Srawley: ASTM STP 410, ASTM, Philadelphia, 1966, pg. 12.

49. M. Smialowski: "The Three Kinds of Embrittlement Effects Produced in Iron and Steels by Hydrogenation". Fundamental Aspects of Stress Corrosion Cracking. Ohio State University, Dept. of Metallurgical Engineering, 1967, pgs. 462-464.

50. M. Smialowski, Z. Szklarska-Smialowski and A. Janko: Omagin. R. Ripan, Acad. Rept. Rumania, Bucharest, 1966, pgs. 541-546.

51. M.L. Wayman and G.C. Smith: "Hydride Formation in Nickel Iron Alloys". J. Phys. Chem. Solids, Vol. 32, 1971, pgs. 103-108.

52. M. Smialowski and A. Szummer: Metallurgia Italiana, Vol. 57, 1965, pgs. 144-155.

53. A. Szummer and A. Janko: "Hydride Phases in Austenitic Stainless Steels". Corrosion, Vol. 35, 1979, pgs. 461-464.

54. D.L. Dull and L. Raymond: "Communications: Surface Cracking of Inconel 718 During Cathodic Charging". Met. Trans., Vol. 4, 1973, pgs. 1635-1640.

55. D. Worthem, I. Robertson, F. Leckie, D. Socie and C. Altstetter: "Inhomogeneous Deformation in INCONEL 718 during monotonic and cyclic loadings". Met. Trans. A., Vol. 21A, 1990, pgs. 3215-3220.

56. H.K. Birnbaum: "Hydrogen-Related Failure Mechanisms in Metals", Environment Sensitive Fracture of Engineering Materials. Z.A. Foroulis, editor. TMS, Warrendale, 1979, pgs 326-361.

57. H.K. Birnbaum: "Hydrogen Related Second Phase Embrittlement of Solids", Hydrogen Embrittlement and Stress Corrosion Cracking. R. Gibala and R.F. Hehemann, editors. ASM, Metals Park, 1984, pgs. 154-177.

58. N.R. Moody, S.L. Robinson and W.M. Garrison, Jr.: "Hydrogen Effects on the Properties and Fracture Modes of Iron-based Alloys". Sandia Report, SAND 88-8860, Sandia National Laboratories, Albuquerque, New Mexico, 87185, Printed July 1989, 95 pages, Accepted for publication in Research Mechanica.

59. W.M. Robertson: "Hydrogen Permeation and Diffusion in Inconel 718 and Incoloy 903". Met. Trans. A., Vol. 8A, 1977, pgs. 1709-1712.